Heliyon 10 (2024) e38206

Contents lists available at ScienceDirect

Heliyon

journal homepage: www.cell.com/heliyon

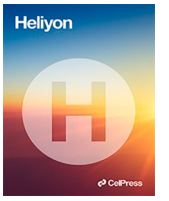

Research article

The effect and mechanism of freeze-dried powder of *Poecilobdella manillensis* on improving inflammatory injury of rat glomerular mesangial cells through TXNIP / NLRP3 pathway

Xi Sun , Maiheliya Mijiti , Chuyin Huang , Shanshan Mei , Kexin Fang , Yaojun Yang *

School of Chinese Materia Medica, Beijing University of Chinese Medicine, Northeast Corner of the Intersection of Yangguang South Street and Baiyang East Road, Fangshan District, Beijing, 102488, China

ARTICLE INFO

Keywords:
Rat mesangial cells
Poecilobdella manillensis freeze-dried powder
NLRP3 inflammasome
Diabetic nephropathy
TXNIP
NLRP3 signaling pathway
Transcriptomics

ABSTRACTS

Objective: Diabetic kidney disease (DKD) is a common complication of *diabetes mellitus*. The pathophysiological changes in platelet function and the hypercoagulable state associated with DKD are closely linked to inflammatory processes. *Poecilobdella manillensis* (PM), a type of leech known for its anticoagulant and antithrombotic properties, has the potential to modulate the inflammatory response in DKD. This study aims to investigate the effect of freeze-dried powder of PM on improving inflammatory injury in rat glomerular mesangial cells and to explore its underlying mechanism.

Methods: Lipopolysaccharide (LPS) stimulated HBZY-1 rat mesangial cells to establish an *in vitro* DKD inflammation model. After the intervention with the water extract of freeze-dried powder of PM (FDPM), cell viability, NO content, and the levels of inflammatory factors such as IL-1β, IL-18, and TNF-α were assessed. Finally, utilizing transcriptomics technology, RT-qPCR, and Western blot methods, the mechanism by which FDPM improves inflammatory injury in rat glomerular mesangial cells was explored and preliminarily validated.

Results: FDPM effectively enhances cell viability and inhibits the production of NO and related inflammatory factors. Transcriptomic analysis suggests that FDPM may exert these effects by regulating the TXNIP/NLRP3 signaling pathway. The mRNA and protein expressions of TXNIP, NLRP3, and MCP-1 in the model cells were reversed by FDPM.

Conclusion: FDPM may improve the micro-inflammatory state of DKD and slow the progression of the disease by regulating the TXNIP/NLRP3 signaling pathway. This study provides a scientific basis for the clinical application of PM DKD treatment.

1. Introduction

Diabetic kidney disease (DKD) also referred to as diabetic nephropathy, is a typical kidney disease caused by *diabetes mellitus* and is a leading cause of end-stage renal disease [1,2]. The number of DKD patients worldwide is increasing annually and is expected to exceed 100 million by 2030 [3,4]. The pathogenesis of DKD includes metabolic abnormalities, hemodynamic disturbances, inflammation, and fibrosis [4,5]. Chronic low-grade inflammation is a key feature of DKD. Growing evidence suggests that immune-mediated micro-inflammation may play a critical role in DKD [6]. Therefore, it is crucial to identify medicines that can suppress the DKD

* Corresponding author.
E-mail address: yangyaoj002@sina.com (Y. Yang).

https://doi.org/10.1016/j.heliyon.2024.e38206
Received 8 July 2024; Received in revised form 19 September 2024; Accepted 19 September 2024
Available online 20 September 2024

micro-inflammatory response through multi-target and multi-pathway mechanisms to effectively treat and delay the progression of DKD.

As a member of the Hirudinidae family, (PM) is a type of leech that has been included in the standard for Chinese medicinal materials in Yunnan Province [7]. Studies have shown that PM, as a blood-sucking leech, contains various active ingredients with anticoagulant, antithrombotic, and anti-inflammatory effects, including bufrudin, hirudin, and their analogs [7–9]. PM has obvious anticoagulant activity, effectively inhibiting thrombin activity, prolonging activated partial thromboplastin time (APTT), thrombin time (TT), and prothrombin time (PT), thereby preventing blood coagulation [10]. Poeciguameri *Poecilobdella manillensis* n is a polypeptide isolated from PM's saliva, a serine protease inhibitor with an anticoagulant domain. It possesses analgesic and antithrombotic activities and can be used to inhibit pain and thrombosis under inflammatory conditions [11]. Previous studies have shown that freeze-drying can effectively retain the anticoagulant activity of PM, making it more practical to use PM in the form of freeze-dried powder [12]. Additionally, related toxicology studies provide strong evidence for the clinical use of freeze-dried powder of PM [13].

During the progression of DKD, pathological conditions such as platelet aggregation and hyperactivity, endothelial dysfunction, and a hypercoagulable state often occur, all of which are associated with the inflammatory response [14,15]. Studies have shown that metabolic disorders and hemodynamic changes in DKD may activate renal micro-inflammation [16]. Therefore, we believe that applying PM to improve the micro-inflammatory state of DKD is feasible due to its anticoagulant and antithrombotic properties.

This study aims to investigate the effect of PM freeze-dried powder (*Poecilobdella manillensis* freeze-dried powder) on improving inflammatory injury in rat mesangial cells and explore its related mechanisms, addressing the current gap in DKD inflammation research related to its treatment. In this research, PM freeze-dried powder was used as the research focus, and its pharmacodynamics were evaluated by establishing an *in vitro* DKD inflammation model, using cell viability and inflammatory factor levels as indicators. Transcriptomic technology and molecular biology experiments were used to explore the mechanism of PM in improving DKD inflammation. This research provides a preliminary scientific basis for clinical workers to apply PM in mitigating the micro-inflammatory response in DKD.

2. Materials and methods

2.1. Preparation of PM freeze-dried powder extract

Preparation of water extract of freeze-dried powder of *Poecilobdella manillensis* (FDPM): 10 g of freeze-dried powder of PM (Yunnan Huazhi Pharmaceutical (Yuanjiang) Co., Ltd., China; Cat. No. 20221207, its composition is provided from supplier and is given as Supplementary Material Fig. S6) was weighed, and deionized water was added at a ratio of 1:5 (w/v). The mixture was stirred and then placed at 4 °C for 24 h, with intermittent stirring. After 24 h, the mixture was centrifuged at 16,000 rpm for 10 min, and the resulting supernatant was lyophilized [17].

2.2. Cell culture

The rat glomerular cell line HBZY-1 (Beijing Union Medical College Cell Culture Center, China) was cultured in low-glucose DMEM medium (Gibco, China; Cat. No. 12320032) supplemented with 1 % penicillin-streptomycin and 10 % fetal bovine serum (CORNING, USA; Cat. Nos. 35-081-CV and 30-009-CI) in a 5 % CO2 incubator at 37 °C (Thermo Fisher Scientific, USA). The cells adhered and proliferated. When the cells reached 70 %–80 %, they were used for passage or experimentation.

2.3. Establishment of in vitro model and screening of administration dose

The cells were seeded at a concentration of 4×10^4 cells/mL and incubated in a cell incubator for 24 h. Once the cells reached 70 % confluence, they were treated with different concentrations of LPS (Sigma Aldrich, USA; Cat. No. SMB00610) at 0.125, 0.25, 0.5, 1, and 2 μg/mL for 12 and 24 h, respectively, with complete medium without LPS serving as the control group. After treatment, cell viability was assessed using a CCK-8 kit (Dalian Meilun Biological Co., Ltd., China; Cat. No. MA0218-1). According to the instructions, absorbance was measured at 450 nm using Epoch 2 TC microplate reader (BioTek, USA) to establish an *in vitro* LPS-induced inflammatory injury model.

Cells were seeded and cultured according to the above method. FDPM was then dissolved in complete medium and administered at concentrations of 0.075,0.15,0.3,0.6,1.2, and 2.4 mg/mL for 12 h. After the intervention, the complete medium was used as the control group, and cell viability was assessed using the CCK-8 method to determine the safe dosage of FDPM.

2.4. Effects of FDPM on LPS-induced injury and inflammation in HBZY-1 cells

To assess the effect of FDPM on LPS-induced injury in HBZY-1 cells, the cells were stimulated with 1 μg/mL LPS for 24 h. Subsequently, the cells in each group were treated for 12 h with either a complete medium without drugs or a complete medium containing FDPM at high (0.3 mg/mL; FDPM-H), medium (0.15 mg/mL; FDPM-M), and low (0.075 mg/mL; FDPM-L) doses. After the intervention, cell viability was assessed, and the cell supernatant was collected for NO content analysis using a NO kit (Beijing Bairuiji Biotechnology Co., Ltd., China; Cat. No. BN27106).

The cells were seeded into 6-well plates at a density of 300,000 cells per well, and LPS and FDPM treatments as described above were initiated when the cells reached 70%–80 % confluence. After treatment, the supernatants from each group were collected and

centrifuged at 4 °C and 4000 rpm for 20 min. The levels of inflammatory factors IL-1β, IL-18, and TNF-α were measured in supernatants using ELISA kits (Quanzhou Jiubang Biotechnology Co., Ltd., China; Cat. Nos. QZ-10037, QZ-10049, and QZ-10160).

2.5. Transcriptome sequencing and analysis

When the cells reached approximately 70 %–80 % confluence, they were stimulated with 1 μg/mL LPS for 24 h, followed by treatment with 0.3 mg/mL FDPM (high dose) for 12 h. Subsequently, cell samples from the control group, model group, and FDPM-H group were sent to Shanghai Meiji Biomedical Technology Co., Ltd. for transcriptome sequencing. Total RNA was extracted from the cells using TRIzol reagent (Invitrogen, USA; Cat. No. 15596026CN), and RNA concentration and purity were assessed. The RNA Quality Number (RQN) was determined using the Agilent 5300 Fragment Analyzer systems (Agilent, USA). Samples with qualified RNA quality were used for cDNA library construction. High-throughput sequencing was performed using the Illumina HiSeq X Ten instrument (Illumina, USA). Quality control was conducted during sequencing to obtain high-quality Clean Reads. Clean Reads were aligned to the reference genome of the rat (*Rattus norvegicus*, reference genome version, Rnor _ 6.0) using HISAT2 software. The DESeq2 software was used to analyze differential gene expression. Genes with $|\log2\ (\text{Fold Change})| \geq 1$, *P*-adjust <0.05 were considered different genes.

The differentially expressed genes (DEGs) identified between the model group and the normal control group, as well as those identified between the FDPM-H treatment group and the model group, were analyzed using a Venn diagram. The intersection of the above two DEGs sets was defined as identical differentially expressed genes (IDEGs). IDEGs were categorized based on their biological processes (BP), cellular components (CC), and molecular functions (MF) using the Gene Ontology (GO) database (http://geneontology.org/). GO enrichment analysis and KEGG (Kyoto Encyclopedia of Genes and Genomes, http://www.genome.jp/kegg/) were conducted on IDEGs with Fisher's exact test. The *P*-values were adjusted by the method of the Benjamini-Hochberg, and it was considered that when $P < 0.05$, there was significant enrichment.

2.6. Quantitative real-time PCR analysis

Cells in the logarithmic growth phase were seeded at a density of 300,000 cells per well. Experimental groups included a blank control, a model group, and three FDPM treatment groups: low-dose (FDPM-L), medium-dose (FDPM-M), and high-dose (FDPM-H). Modeling and drug interventions were conducted according to the methods described previously. TRIzol was used to extract Total RNA from cell samples according to the manufacturer's protocol. Reverse transcription and qPCR were performed according to the instructions provided with the reverse transcription kit and the qPCR kit (Hunan Aikeri Bioengineering Co., Ltd., China; Cat. Nos. AG11707 and AG11701). The RT-qPCR cycle condition included an initial denaturation step at 95 °C for 3 min, followed by 40 cycles of denaturation at 95 °C for 10 s, annealing and extension at 60 °C for 30 s. The PCR primers for the target genes are listed in Table 1, with β-actin serving as the internal reference gene. Gene expression was calculated using the $2^{-\Delta\Delta CT}$ method.

2.7. Western blotting analysis

Similarly, the cells were also divided into five groups after modeling and drug intervention. Pre-cooled RIPA lysis buffer was used to lyse the cells, and protein concentrations were measured using the BCA protein concentration assay kit (Cell Signaling Technology, Inc., USA; Cat. Nos. 9806 and 7780). Equal amounts of protein were separated using SDS-PAGE with a 10 % separation gel and 8 % stacking gel, followed by transfer to an NC membrane (Millipore, Germany). The membrane was blocked with 5 % skimmed milk powder for 1 h at room temperature and then incubated overnight at 4 °C with primary antibodies (TXNIP, NLRP3, β-actin from Zenbio, China; Cat. Nos. 382206, 381207, 380624; MCP-1 from Affinity, China; Cat. No. DF7577). Primary antibodies were diluted according to the manufacturer's instructions. After washing the membrane three times with TBST buffer, it was incubated with the corresponding HRP-labeled secondary antibody (Zenbio, China; Cat. No. 511203). The results were visualized and recorded using a chemiluminescence imaging system (Beijing Liuyi Biotechnology Co., Ltd., China).

2.8. Statistical analysis

Statistical analysis was performed using SPSS 22.0 and GraphPad Prism 8.1 software. Experimental results are presented as the

Table 1
Primer sequence information.

Primer name	primer sequences (5′-3')	primer length (bp)
TXNIP	F:AGTTACCCGAGTCAAAGCCG R:ACTGCTGAGACCCTTGCATC	77
NLRP3	F:AGCTCCTCTGTGAGGGACTT R:CAGCAGGAGTGTGAGGTGAG	88
MCP-1	F:TGATCCCAATGAGTCGGCTG R:TGGACCCATTCCTTATTGGGG	127
β-actin	F:CGCGAGTACAACCTTCTTGC R:CCTTCTGACCCATACCCACC	211

mean ± standard deviation (SD). One-way ANOVA was used for comparisons between groups. A *P*-value of less than 0.05 was considered statistically significant.

3. Results

3.1. Determination of in vitro modeling conditions and dosage

HBZY-1 cells were stimulated with different concentrations of LPS for 12 and 24 h, respectively. As shown in Fig. 1A and B, compared with 12-h stimulation, the cell viability of HBZY-1 cells stimulated for 24 h decreased in a dose-dependent manner. When the concentration of LPS reached 1 μg/mL, the cell inhibition rate after 12 and 24 h exceeded 20 %, with a significant difference ($P < 0.001$). Therefore, 1 μg/mL LPS for 24 h was selected as the modeling condition for subsequent experiments. When the concentration of FDPM reached 0.6 mg/mL, it began to cause severe cellular toxicity compared with the normal control group (Fig. 1C). Consequently, for subsequent experiments, the low, medium, and high dose groups were set at 0.075, 0.15, and 0.3 mg/mL, respectively.

3.2. FDPM improved LPS-induced HBZY-1 cell injury and inflammatory response

The results of the experiment (Fig. 2A–E) showed that the cell viability of the model group was significantly suppressed ($P < 0.001$) compared to the normal group, with an inhibition rate exceeding 25 %, indicating that the model group had stable damage after LPS stimulation. In comparison with the model group, as the dosage of FDPM increased, there was a dose-dependent increase in cell viability, suggesting that FDPM could mitigate LPS-induced injury in HBZY-1 cells. Additionally, NO production in the model group increased significantly ($P < 0.001$) following LPS treatment, accompanied by a notable rise in the levels of IL-1β, IL-18, and TNF-α, known inflammatory factors in the supernatant ($P < 0.001$). After FDPM intervention, these changes were significantly reversed ($P < 0.001$), with FDPM inhibiting the levels of inflammatory factors in a dose-dependent manner.

3.3. Differential gene expression analysis

As shown in Table 2 and Fig. 3B and C, there were 475 DEGs between the model group and the normal control group, with 256 genes upregulated and 219 downregulated. Between the FDPM-H administration group and the model group, there were 874 DEGs, of which 446 were upregulated and 428 were downregulated. To investigate the effect of the intervention of LPS and FDPM-H on HBZY-1 cells, the DEGs from the control group and the model group, as well as those from the FDPM-H administration group and the model group, were analyzed using a Venn diagram (Fig. 3A). This analysis identified 210 common differentially expressed genes (IDEGs), which will be the focus of subsequent analyses.

3.4. GO function annotation and enrichment analysis

According to the results of GO functional annotation (Fig. 4A), IDEGs are classified into 45 secondary functional categories under the GO system. Among the 20 biological process categories, IDEGs primarily concentrate on biological regulation, cellular processes, and response to stimuli. In the 15 cell component categories, IDEGs were significantly concentrated in cell parts, membrane parts, and organelles. Within the 10 molecular function modules, the majority of IDEGs were associated with binding, followed by catalytic activity and molecular function regulation.

A further significant enrichment analysis was conducted on the identified IDEGs. A total of 203 IDEGs were enriched into 1294 secondary functional classes, 309 of which had significant enrichment (*P*-adjust <0.05). Among the 274 biological process categories, the top 20 items (Fig. 4B) included positive regulation of inflammatory response, cell chemotaxis, and positive regulation of immune effector processes, etc. The 10 cell component entries (Fig. 4C) include extracellular space, cell surface, extracellular matrix, etc. The

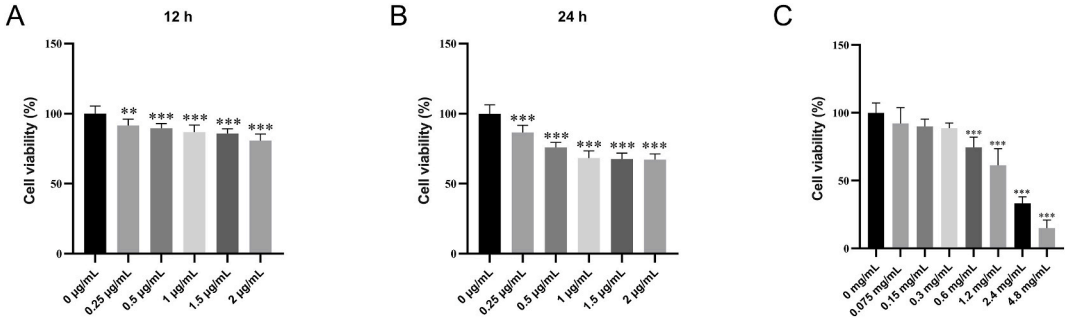

Fig. 1. The *in vitro* modeling conditions and the safe dose range of FDPM. **(A)** Cell inhibition rate after 12 h of intervention with different concentrations of LPS; **(B)** Cell inhibition rate after 24 h of intervention with different concentrations of LPS; **(C)** Screening of the safe dose range of FDPM. ***$P < 0.001$, compared with the normal control group, $n = 6$.

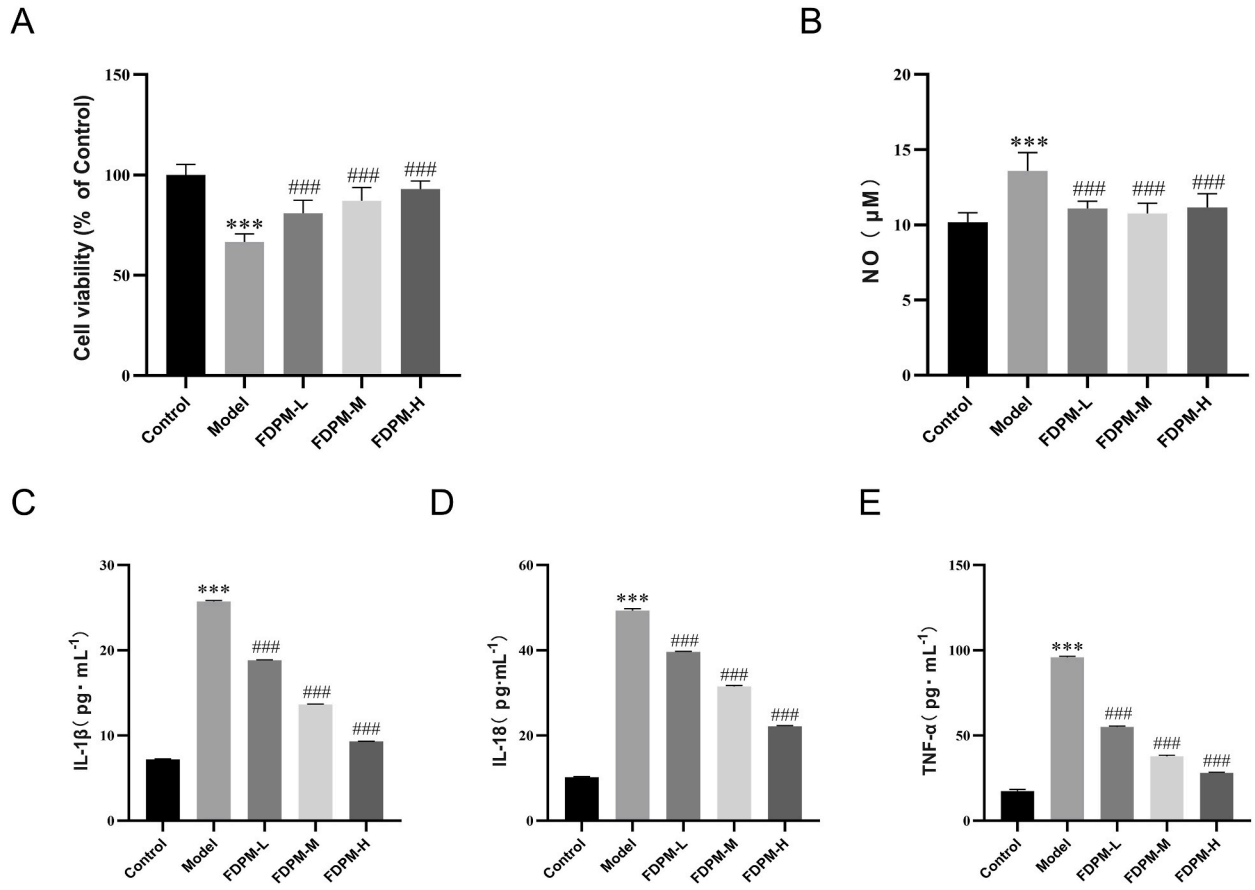

Fig. 2. Effects of FDPM intervention on LPS-induced HBZY-1 cell injury and inflammatory response. **(A)** Effect of FDPM on cell viability following LPS intervention ($n = 6$); **(B)** Effect of FDPM on NO content following LPS intervention ($n = 6$); **(C)** Effect of FDPM on IL-1β levels in cell supernatant following LPS intervention ($n = 3$); **(D)** Effect of FDPM on IL-18 levels in cell supernatant following LPS intervention ($n = 3$); **(E)** Effect of FDPM on TNF-α levels in cell supernatant following LPS intervention ($n = 3$). $^{***}P < 0.001$, compared with the normal control group; $^{\#\#\#}P < 0.001$, compared with the model group.

Table 2
Differentially expressed gene statistics. The treated represents the FDPM-H group.

diff_group	total DEG	up	down
Model_vs_Control	475	256	219
Treated_vs_Model	874	446	428

top 20 items (Fig. 4D) enriched in the molecular functional category included MHC class I protein binding, chemokine receptor binding, metalloendopeptidase activity, etc. Based on the results of GO functional annotation and enrichment analysis, it is speculated that FDPM may improve the injury induced by LPS-induced *in vitro* by regulating cell metabolism, inflammatory responses, and immune function.

3.5. KEGG pathway enrichment analysis

To further explore the changes in the molecular levels of HBZY-1 cells following the intervention of LPS and FDPM-H, KEGG pathway enrichment analysis was performed on the IDEGs. The results showed that a total of 86 IDEGs were enriched into 180 signaling pathways, with 28 pathways showing significant enrichment (P value < 0.05, Supplementary Document Table 1), as shown in Fig. 5. Among these, the IL-17 signaling pathway, TNF signaling pathway, JAK-STAT signaling pathway, NF-kappa B signaling pathway, and NOD-like receptor signaling pathway were selected for further enrichment analysis. The distribution of IDEGs within these pathways was observed. As shown in Fig. 6A and B, genes significantly expressed in the other four pathways were also distributed in the NOD-like receptor signaling pathway, suggesting that this pathway is the main focus of the study. Notably, NLRP3 emerged as the core gene. From the NOD-like receptor signaling pathway map (Supplementary file Figs. S1–2), it was evident that the expression of

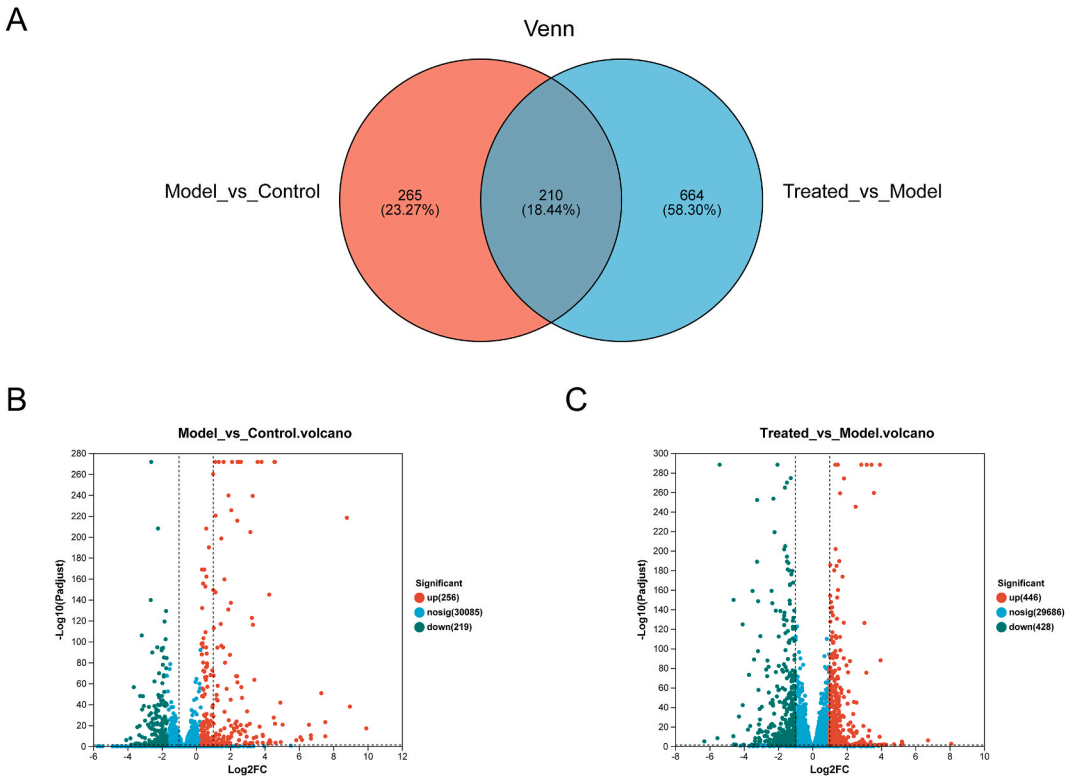

Fig. 3. **(A)** Venn diagram of genes expressed differently; **(B)** Volcanic diagram of difference of expression in model group and normal control group; **(C)** Volcanic diagram of difference of expression in FDPM-H administration group and model group.

NLRP3 and MCP-1 genes increased significantly after LPS stimulation *in vitro*. However, following FDPM-H treatment, the TXNIP, NLRP3, and MCP-1 expression was effectively inhibited.

3.6. FDPM ameliorates LPS-induced cell inflammatory injury by regulating the TXNIP/NLRP pathway

The relative mRNA expression (Fig. 7A–C) and protein expression (Fig. 7D–G) of TXNIP, NLRP3, and MCP-1 were measured across all groups. The results showed that both mRNA and protein expression levels of these markers were significantly higher in the model group compared to the control group ($P < 0.001$ for mRNA, $P < 0.05$ for protein). However, treatment with different doses of FDPM significantly reversed these changes to varying degrees, suggesting that FDPM effectively inhibits the LPS-induced mRNA and protein expression of TXNIP, NLRP3, and MCP-1 in HBZY-1 cells.

4. Discussion

Growing evidence suggests that the occurrence of DKD is not only linked to abnormal hemorheology and hyperglycemia but also to the activation of innate immune system activation and persistent micro-inflammatory state in diabetic patients [18,19]. As a result, chronic micro-inflammation, driven by the infiltration of immune cells and cytokines into renal tissue, has gradually emerged as a significant hallmark of DKD. Drugs that target innate immune signaling pathways and inflammatory signaling pathways may offer therapeutic potential for DKD [20]. The anticoagulant and anti-inflammatory properties of hirudin are closely related to the treatment of diabetes and its complications [21,22]. PM contains bufrudin, hirudin, and hirudin analogs [8,23], making it a promising candidate for treating DKD.

To investigate the protective effects of FDPM against inflammatory injury of glomerular mesangial cells during DKD treatment, this study established an inflammatory injury model *in vitro* [24] by using the LPS to stimulate glomerular mesangial cells, thereby mimicking the inflammatory environment of glomerular mesangial cells in diabetic nephropathy. Our findings demonstrated that FDPM can improve LPS-induced cell injury, significantly inhibiting the production and release of IL-1β, IL-18, TNF-α, and NO, which suggests that FDPM possesses notable anti-inflammatory properties. Transcriptomics, a research method that explores the transcriptional activities and regulatory mechanisms of cells or genes at a comprehensive level [25], has become an increasingly popular approach for studying disease pathology and the pharmacodynamic mechanism of traditional Chinese medicine [26]. To explore the molecular mechanism underlying FDPM 's effects on LPS-induced inflammatory injury in HBZY-1 cells *in vitro*, we identified 210 IDEGs by high-throughput transcriptome sequencing.

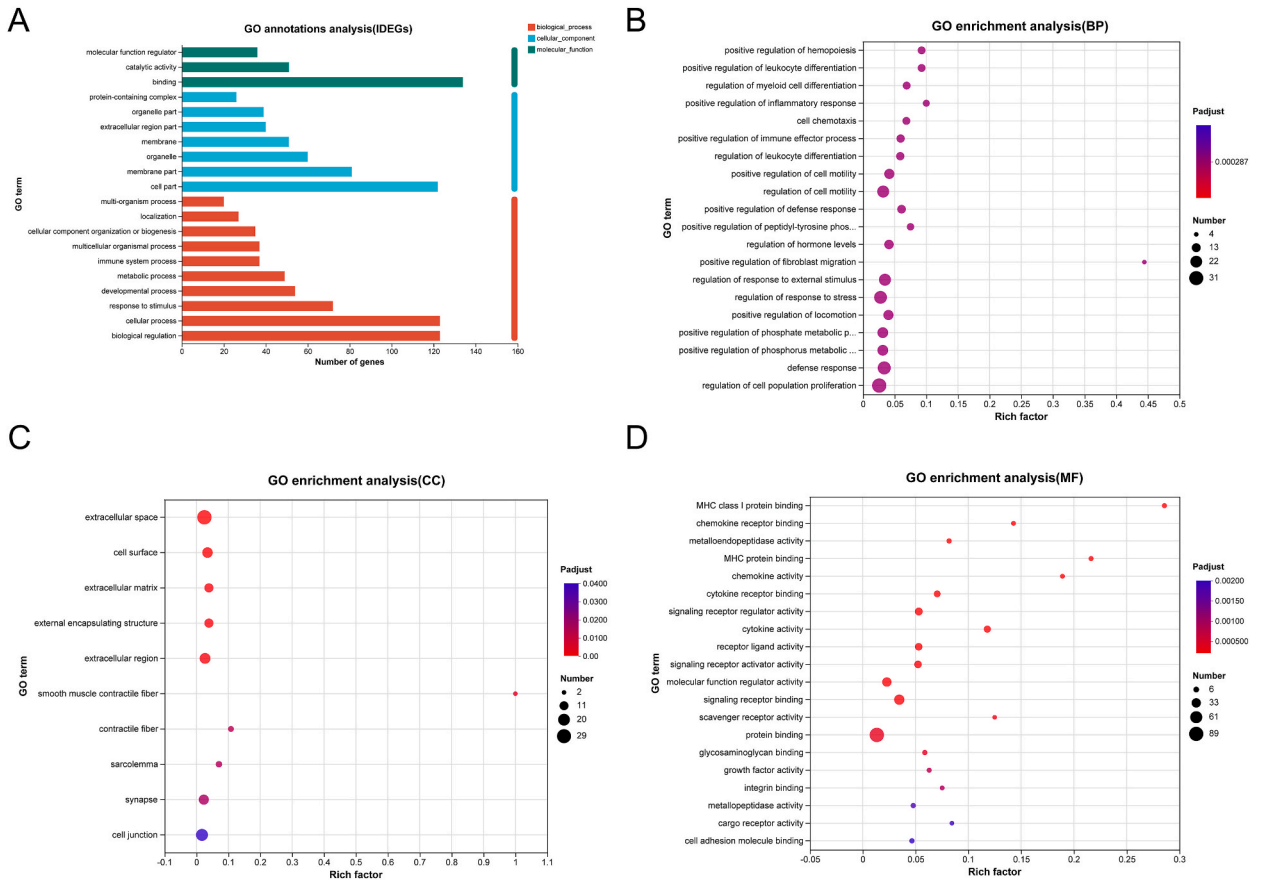

Fig. 4. **(A)** GO function secondary classification annotation of IDEGs; **(B)** IDEGs were enriched in the first 20 items of biological processes (BP); **(C)** IDEGs were enriched in the top 20 items of cellular components (CC); **(D)** IDEGs were enriched in the first 20 items of molecular functions (MF).

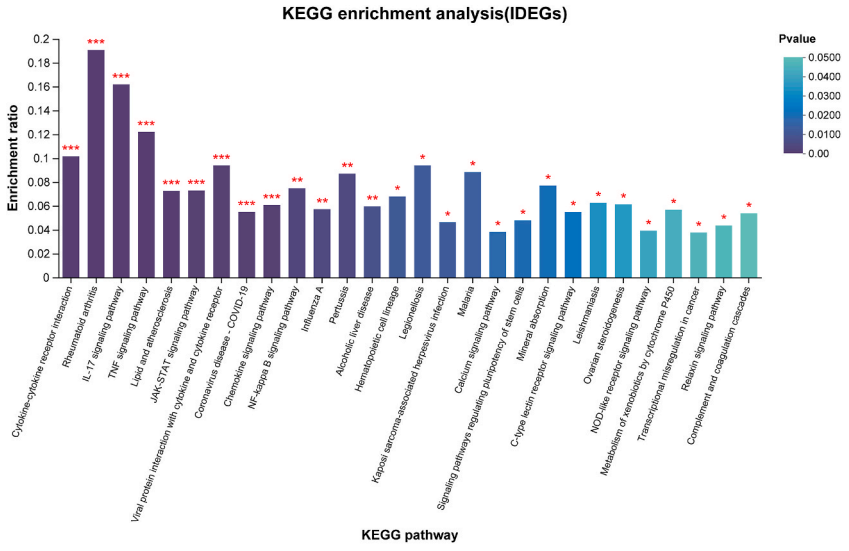

Fig. 5. KEGG enrichment analysis of IDEGs.

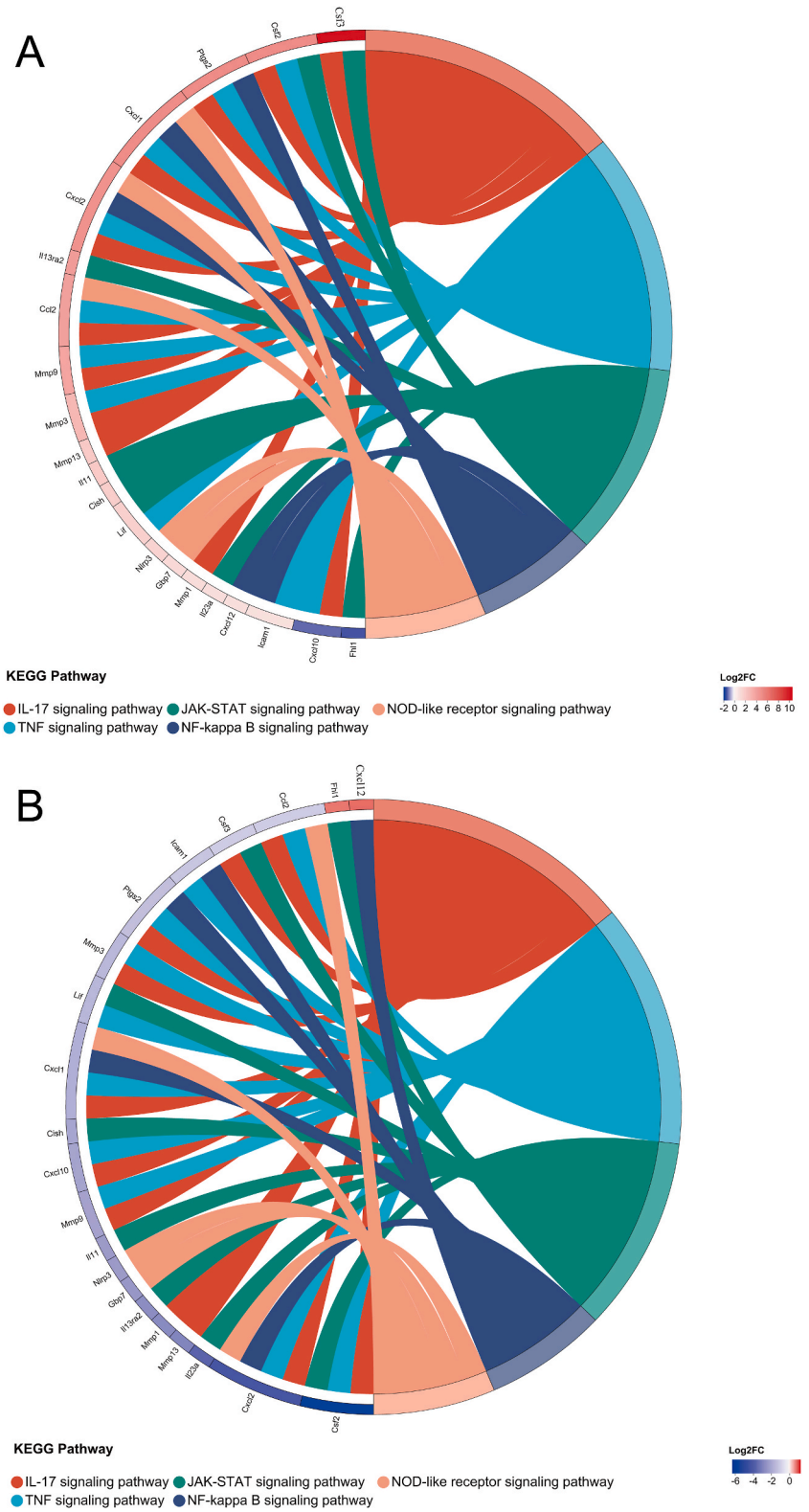

Fig. 6. **(A)** KEGG pathway enrichment chord diagram comparing the model group with the normal control group; **(B)** KEGG pathway enrichment chord diagram comparing the FDPM-H administration group with the model group. On the right side, the pathway information related to significant enrichment of the differential genes is displayed. On the left side, the pathway genes are sorted by log2FC in descending order.

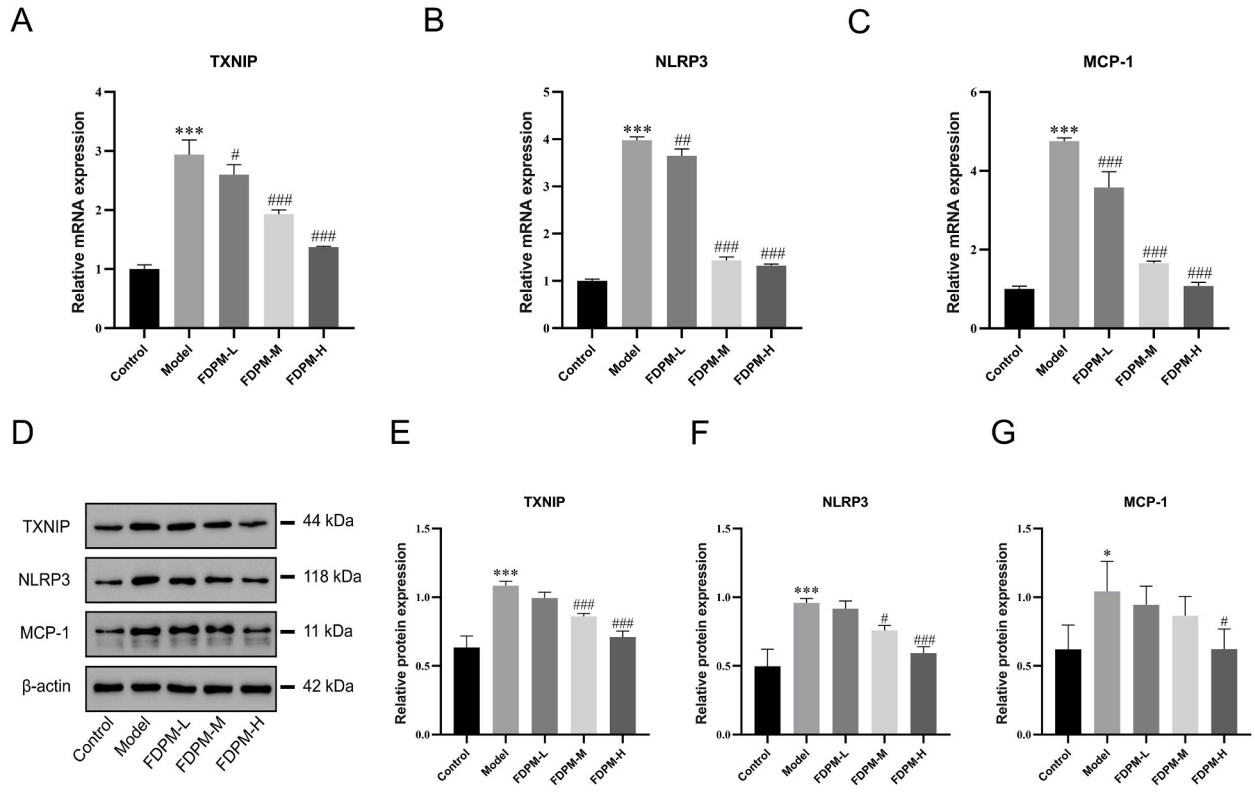

Fig. 7. Effects of FDPM on TXNIP/NLRP pathway in LPS-induced cellular inflammatory injury. **(A)** Relative expression of TXNIP mRNA in each group; **(B)** Relative expression of NLRP3 mRNA in each group; **(C)** Relative expression of MCP-1 mRNA in each group; **(D)** Western blot bands of TXNIP, NLRP3, and MCP-1 proteins; **(E)** Relative content of TXNIP protein in each group; **(F)** Relative content of NLRP3 protein in each group; **(G)** Relative content of MCP-1 protein in each group. $^{*}P < 0.05$, $^{***}P < 0.001$, compared with the normal control group; $^{\#}P < 0.05$, $^{\#\#}P < 0.01$, $^{\#\#\#}P < 0.001$, compared with the model group, $n = 3$. The original Western blot bands are shown in Figs. S3(A–D)-S5 (A–D) in the supplemental file.

Numerous studies have demonstrated a close association between the TXNIP/NLRP3 signaling pathway and DKD. *In vitro*, LPS stimulation of glomerular mesangial cells has been shown to induce the expression and release of TXNIP, NLRP3, IL-1β, TNF-α, and IL-18 in a dose-dependent and time-dependent manner, indicating that LPS can trigger inflammation and exacerbate renal damage through the TXNIP/NLRP3 pathway [24]. Similarly, research has revealed that punicalagin can mitigate the inflammatory state of diabetic nephropathy by establishing a diabetic mouse model, potentially through the down-regulation of NOX4 expression and inhibition of pyroptosis mediated by the TXNIP/NLRP3 pathway [27]. Additionally, Schizandrin A has been found to inhibit the expression of TXNIP and NLRP3 proteins in DKD mice, reducing IL-1β levels in the kidneys and thereby offering renal protection [28]. Furthermore, by blocking the TXNIP/NLRP3 inflammatory pathway in diabetic nephropathy, vitamin D3 has been shown to protect renal tubular epithelial cells from fibrosis and apoptosis [29]. Therefore, based on previous studies, the TXNIP/NLRP3 axis in the NOD-like receptor signaling pathway was selected as the target pathway for this investigation.

The NLRP3 inflammasome, composed of NLRP3, ASC, and pro-caspase-1, is a crucial component of the innate immune system, playing an essential role in DKD [30,31]. In glomerular mesangial cells affected by DKD, the NLRP3 inflammasome can be activated by hyperglycemia, oxidative stress, and other factors, leading to an inflammatory response that exacerbates glomerular damage [32]. During the formation of NLRP3 inflammasome, pro-Caspase-1 is recruited and cleaved to produce active Caspase-1, which then promotes the conversion of pro-IL-1β and pro-IL-18 into the active pro-inflammatory cytokines IL-1β and IL-18, thereby triggering immune response [33]. TXNIP, an early gene inducible by diabetes and hyperglycemia [34,35], is critical for NLRP3 inflammasome activation [36,37]. In the context of diabetes and oxidative stress, TXNIP plays a vital role in innate immunity by activating the NLRP3 inflammasome and facilitating the release of IL-1β [38]. Renal exposure to stimuli such as lipopolysaccharide or high glucose is known to activate the NLRP3 inflammasome, or promote the binding of TXNIP to the NLRP3 inflammasome, leading to the release of IL-1β and IL-18, thereby exacerbating the inflammation response associated with diabetic nephropathy [39,40].

During DKD, there is an increase in the levels of inflammatory cytokines such as IL-1β, IL-18, TNF-α, and MCP-1 in the kidney [41]. IL-1β, a key inflammatory mediator, is involved in cellular activity and immune response regulation [42]. It can also impair the kidney's filtration function by damaging the junctions and adhesions of glomerular endothelial cells [43]. IL-18 participates in adaptive immunity by regulating T-cell activation and differentiation [44]. As another important inflammatory factor in the kidney, IL-18 induces the expression of pro-inflammatory and oxidative stress-related genes [45], while also mediating the production of other inflammatory factors [46]. TNF-α, highly expressed in the blood and urine of diabetic patients, acts as a pro-inflammatory factor,

influencing the recruitment and activation of leukocytes, thereby exacerbating inflammation and DKD [47]. Additionally, prolonged TNF-α activity promotes the secretion of IL-1, IL-6, and IL-8, further aggravating the inflammatory response [48]. MCP-1, mainly produced by activated monocytes/macrophages [49], plays a critical role in recruiting these cells to the glomeruli, making it an essential component of the inflammatory response [50]. In DKD, MCP-1 is produced by mesangial cells and is recognized as a key mediator in the disease's inflammatory process [51,52]. Its expression can be increased by high glucose levels and glycated albumin [53], and additional stimuli, such as TNF-α, can further promote MCP-1 expression [54].

5. Conclusions

Our study demonstrated that FDPM intervention could significantly reduce the mRNA and protein expression levels of TXNIP and NLRP3 following LPS-induced inflammatory injury in mesangial cells. Additionally, it decreased the expression levels of relevant pro-inflammatory factors IL-18, IL-1β, and TNF-α, while also significantly inhibiting MCP-1, a downstream target of these inflammatory factors. Based on these findings, we speculate that FDPM may inhibit the inflammatory cascade triggered by the NLRP3 inflammasome by regulating the TXNIP/NLRP3 pathway, thereby improving the micro-inflammatory response in DKD. In summary, our study has investigated the molecular mechanism of freeze-dried powder of PM in treating DKD, addressing gaps in research on the pharmacological activity and molecular mechanism of PM, and providing a further basis for the clinical application of PM in DKD treatment.

Data availability statement

Datasets generated and/or analyzed during the current study can be found in the Gene Expression Omnibus (GEO) repository (https://www.ncbi.nlm.nih.gov/geo/), GSE270526. To review GEO accession GSE270526: Go to https://www.ncbi.nlm.nih.gov/geo/query/acc.cgi?acc=GSE270526.

Enter token qtmfkuqknvyblsr into the box.

Funding statement

The authors gratefully acknowledge financial support from the Natural Science Foundation of Beijing Municipality (No. 7222275).

CRediT authorship contribution statement

Xi Sun: Writing – review & editing, Writing – original draft, Formal analysis, Data curation, Conceptualization. **Maiheliya Mijiti:** Writing – original draft, Investigation, Data curation, Conceptualization. **Chuyin Huang:** Investigation, Formal analysis, Data curation. **Shanshan Mei:** Investigation, Formal analysis, Data curation. **Kexin Fang:** Investigation, Formal analysis, Data curation. **Yaojun Yang:** Project administration, Methodology, Funding acquisition, Conceptualization.

Declaration of competing interest

The authors declare that they have no known competing financial interests or personal relationships that could have appeared to influence the work reported in this paper.

Appendix A. Supplementary data

Supplementary data to this article can be found online at https://doi.org/10.1016/j.heliyon.2024.e38206.

References

[1] H.A. Uchida, H. Nakajima, M. Hashimoto, A. Nakamura, T. Nunoue, K. Murakami, et al., Efficacy and safety of esaxerenone in hypertensive patients with diabetic kidney disease: a multicenter, open-label, prospective study, Adv. Ther. 39 (11) (2022) 5158–5175, https://doi.org/10.1007/s12325-022-02294-z.
[2] J. Chang, J.S. Zheng, X. Gao, H.B. Dong, H.T. Yu, M. Huang, et al., TangShenWeiNing formula prevents diabetic nephropathy by protecting podocytes through the SIRT1/HIF-1α pathway, Front. Endocrinol. 13 (2022), https://doi.org/10.3389/fendo.2022.888611.
[3] L.X. Tang, B. Wei, L.Y. Jiang, Y.Y. Ying, K. Li, T.X. Chen, et al., Intercellular mitochondrial transfer as a means of revitalizing injured glomerular endothelial cells, World J, Stem Cell. 14 (9) (2022) 729–743, https://doi.org/10.4252/wjsc.v14.i9.729.
[4] R.Z. Alicic, M.T. Rooney, K.R. Tuttle, Diabetic kidney disease, clin, J. Am. Soc. Nephrol. 12 (12) (2017) 2032–2045, https://doi.org/10.2215/CJN.11491116.
[5] Y. Wang, Z. Sui, M. Wang, P. Liu, Natural products in attenuating renal inflammation via inhibiting the NLRP3 inflammasome in diabetic kidney disease, Front. Immunol. 14 (2023), https://doi.org/10.3389/fimmu.2023.1196016.
[6] R.B. Zhou, A. Tardivel, B. Thorens, I. Choi, J. Tschopp, Thioredoxin-interacting protein links oxidative stress to inflammasome activation, Nat. Immunol. 11 (2) (2010) 136–140, https://doi.org/10.1038/ni.1831.
[7] Y. Li, F.G. Gu, T.T. Guo, T.C. Lu, W.A. Xu, H.Y. Han, Study on the active components of anticoagulant extract of Poecilobdella manillensis, Chin. Med. Mat. 44 (12) (2021) 2850–2855, https://doi.org/10.13863/j.issn1001-4454.2021.12.021 (in Chinese).
[8] Q.Y. Huang, J.Y. Tang, X.X. Chai, W. Ren, J.B. Wang, Q.C. Gan, et al., Affinity ultrafiltration and UPLC-HR-Orbitrap-MS based screening of thrombin-targeted small molecules with anticoagulation activity from Poecilobdella manillensis, J. Chromatogr. B 1178 (2021) 122822, https://doi.org/10.1016/j.jchromb.2021.122822.

[9] P. Lukas, R. Wolf, B.H. Rauch, J. Hildebrandt, C. Müller, Hirudins of the Asian medicinal leech, Hirudinaria manillensis: same same, but different, Parasitol. Res. 118 (7) (2019) 2223–2233, https://doi.org/10.1007/s00436-019-06365-z.

[10] Y.Z. Ding, T.X. Duan, Y. Shan, X.F. Wang, H. Yang, R.J. Yuan, Comparative studies on anti-thrombin activity and anticoagulant mechanism between whitmania PigraWhitman and hirudinaria manillensis, China Pharm. 19 (9) (2016) 1621–1624 (in Chinese).

[11] C.M. Wang, M.R. Chen, X.Y. Lu, S. Yang, M. Yang, Y.Q. Fang, et al., Isolation and characterization of poeciguamerin, a peptide with dual analgesic and anti-thrombotic activity from the Poecilobdella manillensis leech, Int. J. Mol. Sci. 24 (13) (2023) 11097, https://doi.org/10.3390/ijms241311097.

[12] M. Zhong, Y. Lei, Y. Li, H. Tan, Y. Shan, R.J. Yuan, Study on anticoagulant activity of different processed products of whitmania pigra whitman and hirudinaria manillensis lesson *in vivo*, J. Chin. Med. Mater. 43 (6) (2020) 1351–1353, https://doi.org/10.13863/j.issn1001-4454.2020.06.012 (in Chinese).

[13] Y.J. Zhang, C.X. Zhang, C. Li, J.L. Yang, N. Pi, T.T. Niu, et al., Repeated administration toxicity of study freeze-dried powder of Poecilobdella manillensis, J. Yunnan Minzu Univ. (nat. Sci. Ed.) 33 (2) (2024) 169–177 (in Chinese).

[14] Y. Takeda, K. Matoba, K. Sekiguchi, Y. Nagai, T. Yokota, K. Utsunomiya, et al., Endothelial dysfunction in diabetes, Biomedicines 8 (7) (2020) 182, https://doi.org/10.3390/biomedicines8070182.

[15] U.J. Rustiasari, J.J. Roelofs, The role of platelets in diabetic kidney disease, Int. J. Mol. Sci. 23 (15) (2022) 8270, https://doi.org/10.3390/ijms23158270.

[16] K. Shikata, H. Makino, Microinflammation in the pathogenesis of diabetic nephropathy, J. Diabetes Investig. 4 (2) (2013) 142–149, https://doi.org/10.1111/jdi.12050.

[17] X.F. Wang, Y.K. Sun, R.C. Lin, Y.R. Feng, W.T. Zhang, H.L. Xie, et al., Comparison of the effects on angiogenesis activity between whitmania pigra whitman and hirudinaria manillensis lesson based on a zebrafish model, China Pharm. 20 (12) (2017) 2099–2103 (in Chinese).

[18] R. Pérez-morales, M. Del pino, J. Valdivielso, A. Ortiz, C. Mora-fernández, J. Navarro-gonzález, Inflammation in diabetic kidney disease, Nephron 143 (1) (2019) 12–16, https://doi.org/10.1159/000493278.

[19] J.C. Pickup, Inflammation and activated innate immunity in the pathogenesis of type 2 diabetes, Diabetes Care 27 (3) (2004) 813–823, https://doi.org/10.2337/diacare.27.3.813.

[20] S.C.W. Tang, W.H. Yiu, Innate immunity in diabetic kidney disease, Nat. Rev. Nephrol. 16 (4) (2020) 206–222, https://doi.org/10.1038/s41581-019-0234-4.

[21] X.X. Pang, Y.G. Zhang, Z.N. Peng, X.J. Shi, J.R. Han, Y.F. Xing, Hirudin reduces nephropathy microangiopathy in STZ-induced diabetes rats by inhibiting endothelial cell migration and angiogenesis, Life Sci. 255 (2020) 117779, https://doi.org/10.1016/j.lfs.2020.117779.

[22] F. Tian, X. Yi, F.F. Yang, Y. Chen, W.H. Zhu, P. Liu, et al., Research progress on the treatment of diabetic nephropathy with leech and its active ingredients, Front. Endocrinol. 15 (2024), https://doi.org/10.3389/fendo.2024.1296843.

[23] M. Alaama, O. Kucuk, B. Bilir, A. Merzouk, A.M. Ghawi, M.B. Yerer, et al., Development of Leech extract as a therapeutic agent: a chronological review, Pharmacol. Res. Mod. Chin. Med. 10 (2024) 100355, https://doi.org/10.1016/j.prmcm.2023.100355.

[24] H. Feng, J.L. Gu, F. Gou, W. Huang, C.L. Gao, G. Chen, et al., High glucose and lipopolysaccharide prime NLRP3 inflammasome via ROS/TXNIP pathway in mesangial cells, J. Diabetes Res. 2016 (2016) 1–11, https://doi.org/10.1155/2016/6973175.

[25] V. Gomase, S. Tagore, Transcriptomics, Curr. Drug Metabol. 9 (3) (2008) 245–249, https://doi.org/10.2174/138920008783884759.

[26] Y.F. Liu, N. Ai, J. Liao, X.H. Fan, Transcriptomics: a sword to cut the gordian knot of traditional Chinese medicine, Biomarkers Med. 9 (11) (2015) 1201–1213, https://doi.org/10.2217/bmm.15.91.

[27] X. An, Y.H. Zhang, Y. Cao, J.H. Chen, H. Qin, L.N. Yang, Punicalagin protects diabetic nephropathy by inhibiting pyroptosis based on TXNIP/NLRP3 pathway, Nutrients 12 (5) (2020) 1516, https://doi.org/10.3390/nu12051516.

[28] X.H. Wang, Q. Li, B.Z. Sui, M.D. Xu, Z.C. Pu, T. Qiu, Schisandrin A from schisandra chinensis attenuates ferroptosis and NLRP3 inflammasome-mediated pyroptosis in diabetic nephropathy through mitochondrial damage by AdipoR1 ubiquitination, Oxid. Med. Cell. Longev. 2022 (2022) 1–23, https://doi.org/10.1155/2022/5411462.

[29] G.Q. Li, S.H. He, T. Liu, N. Zheng, Therapeutic potential of vitamin D3 in mitigating high glucose-induced renal damage: mechanistic insights into oxidative stress inhibition and TXNIP/NLRP3 signaling pathway blockade, Exp. Ther. Med. 28 (1) (2024), https://doi.org/10.3892/etm.2024.12565.

[30] R. Ramachandran, A. Manan, J. Kim, S. Choi, NLRP3 inflammasome: a key player in the pathogenesis of life-style disorders, Exp. Mol. Med. 56 (7) (2024) 1488–1500, https://doi.org/10.1038/s12276-024-01261-8.

[31] J.Y. Jin, M.Z. Zhang, Exploring the role of NLRP3 inflammasome in diabetic nephropathy and the advancements in herbal therapeutics, Front. Endocrinol. 15 (2024), https://doi.org/10.3389/fendo.2024.1397301.

[32] Y.Y. Qiu, L.Q. Tang, Roles of the NLRP3 inflammasome in the pathogenesis of diabetic nephropathy, Pharmacol. Res. 114 (2016) 251–264, https://doi.org/10.1016/j.phrs.2016.11.004.

[33] T. Jourdan, G. Godlewski, R. Cinar, A. Bertola, G. Szanda, J. Liu, et al., Activation of the Nlrp3 inflammasome in infiltrating macrophages by endocannabinoids mediates beta cell loss in type 2 diabetes, Nat. Med. 19 (9) (2013) 1132–1140, https://doi.org/10.1038/nm.3265.

[34] L. Perrone, T.S. Devi, K. Hosoya, T. Terasaki, L.P. Singh, Thioredoxin interacting protein (TXNIP) induces inflammation through chromatin modification in retinal capillary endothelial cells under diabetic conditions, J. Cell. Physiol. 221 (1) (2009) 262–272, https://doi.org/10.1002/jcp.21852.

[35] T. Beothe, J. Docs, G. Kovacs, L. Peterfi, Increased level of TXNIP and nuclear translocation of TXN is associated with end stage renal disease and development of multiplex renal tumours, BMC Nephrol. 25 (1) (2024), https://doi.org/10.1186/s12882-024-03653-4.

[36] R.B. Zhou, A. Tardivel, B. Thorens, I. Choi, J. Tschopp, Thioredoxin-interacting protein links oxidative stress to inflammasome activation, Nat. Immunol. 11 (2) (2010) 136–140, https://doi.org/10.1038/ni.1831.

[37] X.S. Xi, R. Zhang, Y.J. Chi, Z.M. Zhu, R.F. Sun, W.J. Gong, TXNIP regulates NLRP3 inflammasome-induced pyroptosis related to aging via cAMP/PKA and PI3K/akt signaling pathways, Mol. Neurobiol. (2024), https://doi.org/10.1007/s12035-024-04089-5.

[38] K. Schroder, R. Zhou, J. Tschopp, The NLRP3 inflammasome: a sensor for metabolic danger? Science 327 (5963) (2010) 296–300, https://doi.org/10.1126/science.1184003.

[39] P. Gao, X.F. Meng, H. Su, F.F. He, S. Chen, H. Tang, et al., Thioredoxin-interacting protein mediates NALP3 inflammasome activation in podocytes during diabetic nephropathy, Biochim. Biophys. Acta Mol. Cell Res. 1843 (11) (2014) 2448–2460, https://doi.org/10.1016/j.bbamcr.2014.07.001.

[40] R. Stienstra, C. Tack, T. Kanneganti, L. Joosten, M. Netea, The inflammasome puts obesity in the danger zone, Cell Metabol. 15 (1) (2012) 10–18, https://doi.org/10.1016/j.cmet.2011.10.011.

[41] H.Y. Chen, X.R. Huang, W.S. Wang, J.H. Li, R.L. Heuchel, A.C. Chung, et al., The protective role of Smad7 in diabetic kidney disease: mechanism and therapeutic potential, Diabetes 60 (2) (2011) 590–601, https://doi.org/10.2337/db10-0403.

[42] G. Lopez-castejon, D. Brough, Understanding the mechanism of IL-1β secretion, Cytokine Growth Factor Rev. 22 (4) (2011) 189–195, https://doi.org/10.1016/j.cytogfr.2011.10.001.

[43] L.N. Du, F.Y. Dong, L. Guo, Y.L. Hou, F. Yi, J. Liu, et al., Interleukin-1β increases permeability and upregulates the expression of vascular endothelial-cadherin in human renal glomerular endothelial cells, Mol. Med. Rep. 11 (5) (2015) 3708–3714, https://doi.org/10.3892/mmr.2015.3172.

[44] K. Futosi, S. Fodor, A. Mócsai, Reprint of Neutrophil cell surface receptors and their intracellular signal transduction pathways, Int. Immunopharm. 17 (4) (2013) 1185–1197, https://doi.org/10.1016/j.intimp.2013.11.010.

[45] N.M. Elsherbiny, M.M. Al-gayyar, The role of IL-18 in type 1 diabetic nephropathy: the problem and future treatment, Cytokine 81 (2016) 15–22, https://doi.org/10.1016/j.cyto.2016.01.014.

[46] W.T. He, H.Q. Wan, L.C. Hu, P.D. Chen, X. Wang, Z. Huang, et al., Gasdermin D is an executor of pyroptosis and required for interleukin-1β secretion, Cell Res. 25 (12) (2015) 1285–1298, https://doi.org/10.1038/cr.2015.139.

[47] Y.L. Chen, Y.C. Qiao, Y. Xu, W. Ling, Y.H. Pan, Y.C. Huang, et al., Serum TNF-α concentrations in type 2 *diabetes mellitus* patients and diabetic nephropathy patients: a systematic review and meta-analysis, Immunol. Lett. 186 (2017) 52–58, https://doi.org/10.1016/j.imlet.2017.04.003.

[48] R. Neta, T.J. Sayers, J.J. Oppenheim, Relationship of TNF to interleukins, Immunol. 56 (1992) 499–566.

[49] S.Y. Lim, A.E. Yuzhalin, A.N. Gordon-weeks, R.J. Muschel, Targeting the CCL2-CCR2 signaling axis in cancer metastasis, Oncotarget 7 (19) (2016) 28697–28710, https://doi.org/10.18632/oncotarget.7376.

[50] R. Coppo, Proteasome inhibitors in progressive renal diseases, Nephrol, Dial. Transplant. 29 (2014) i25–i30, https://doi.org/10.1093/ndt/gft271.
[51] S. Giunti, G.H. Tesch, S. Pinach, D.J. Burt, M.E. Cooper, P. Cavallo-perin, et al., Monocyte chemoattractant protein-1 has prosclerotic effects both in a mouse model of experimental diabetes and *in vitro* in human mesangial cells, Diabetologia 51 (1) (2008) 198–207, https://doi.org/10.1007/s00125-007-0837-3.
[52] J.F. Navarro-gonzález, C. Mora-fernández, M.M.D. Fuentes, J. García-pérez, Inflammatory molecules and pathways in the pathogenesis of diabetic nephropathy, Nat. Rev. Nephrol. 7 (6) (2011) 327–340, https://doi.org/10.1038/nrneph.2011.51.
[53] C.G. Ihm, J.K. Park, S.P. Hong, T.W. Lee, B.S. Cho, M.J. Kim, et al., A high glucose concentration stimulates the expression of monocyte chemotactic peptide 1 in human mesangial cells, Nephron 79 (1) (1998) 7–33, https://doi.org/10.1159/000044988.
[54] C.J. Lockwood, P. Matta, G. Krikun, L.A. Koopman, R. Masch, P. Toti, et al., Regulation of monocyte chemoattractant protein-1 expression by tumor necrosis factor-α and interleukin-1β in first trimester human decidual cells, Am. J. Pathol. 168 (2) (2006) 445–452, https://doi.org/10.2353/ajpath.2006.050082.